

Populating the Galaxy with Low-mass X-ray Binaries

Paul D. Kiel^{1,2*} and Jarrod R. Hurley²

¹Centre for Astrophysics and Supercomputing, Swinburne University of Technology, Hawthorn, Victoria, 3122, Australia
²Department of Mathematics, PO Box 28M, Monash University, Victoria 3800, Australia

Accepted xxx. Received xxx; in original form xxx

ABSTRACT

We perform binary population synthesis calculations to investigate the incidence of low-mass X-ray binaries and their birth rate in the Galaxy. We use a binary evolution algorithm that models all the relevant processes including tidal circularization and synchronization. Parameters in the evolution algorithm that are uncertain and may affect X-ray binary formation are allowed to vary during the investigation. We agree with previous studies that under standard assumptions of binary evolution the formation rate and number of black-hole low-mass X-ray binaries predicted by the model are more than an order of magnitude less than what is indicated by observations. We find that the common-envelope process cannot be manipulated to produce significant numbers of black-hole low-mass X-ray binaries. However, by simply reducing the mass-loss rate from helium stars adopted in the standard model, to a rate that agrees with the latest data, we produce a good match to the observations. Including low-mass X-ray binaries that evolve from intermediate-mass systems also leads to favourable results. We stress that constraints on the X-ray binary population provided by observations are used here merely as a guide as surveys suffer from incompleteness and much uncertainty is involved in the interpretation of results.

Key words: binaries: close – stars: evolution – stars: low-mass – stars: neutron – Galaxy: stellar content – X-rays: binaries

1 INTRODUCTION

X-ray binaries (XBs) are close binary systems that typically have luminosities in excess of 10^{35} erg s $^{-1}$ (Cowley et al. 1987) with radiation peaked strongly in the X-ray region. They are composed of a compact star – black hole (BH) or neutron star (NS) – accreting matter from a non-compact companion. X-ray binary systems are traditionally divided into sub classes according to the mass of the donor star, M_d . High-mass X-ray binaries (HMXBs) have $M_d > 10M_\odot$ while low-mass X-ray binaries (LMXBs) have $M_d < 2M_\odot$ and intermediate-mass X-ray binaries (IMXBs) complete the classification picture. Observationally LMXBs are distinguished from HMXBs, because in comparison their spectra are devoid of normal stellar absorption features (Ritter & Kolb 2003). This is thought to be the result of the donor star being overwhelmed by an accretion disk and therefore information from the star is lost (Ritter & Kolb 2003).

Detailed X-ray surveys have discovered 150 known LMXBs in our Galaxy (Liu, van Paradijs & van den Heuvel 2001). For a subset of these, dynamical mass estimates are available and reveal that at least 18 are BH-LMXBs (Orosz et al. 2004). Empirical estimates based on these surveys

and taking into account selection effects suggest that the total number of BH-LMXBs in our Galaxy is in the order of 1700 (Romani 1998; Kalogera 1999). The observations also indicate that the formation rates of NS-LMXBs and BH-LMXBs are similar (Cowley 1992; Portegies Zwart, Verbunt & Ergma 1997) and of the order of 10^{-7} yr $^{-1}$ (Kalogera 1999; Pfahl, Rappaport & Podsiadlowski 2003). However, as previously noted by Kalogera & Webbink (1998) the current state of the observational data provides only limited constraints as the data suffers from incompleteness and selection effects which are poorly understood. Chief among these is the need to compensate for the potential transient behaviour of the LMXB sources which can produce variability on timescales as low as days (Chen, Scrader & Livio 1997). Until we have a better understanding of the selection effects the empirical estimates can only be used as a general guide to the properties of the Galactic LMXB population. Even so, these estimates have been used as constraints on models of LMXB formation in the past. To date population synthesis studies have found it difficult to reproduce the suggested numbers and the formation rate of BH-LMXBs, especially as standard forms of the initial mass function make BH progenitors much rarer than NS progenitors (e.g. Portegies Zwart, Verbunt & Ergma 1997; Podsiadlowski, Rappaport & Han 2003). An associated problem is that the observed Galac-

* E-mail: pkiel@astro.swin.edu.au (PDK)

tic birthrate of binary millisecond pulsars (BMPs) is about 10^{-5} yr^{-1} (Lorimer 1995) – two orders of magnitude greater than the inferred birthrate of LMXBs which are thought to create BMPs (Kulkarni & Narayan 1988). Recently Pfahl, Rappaport & Podsiadlowski (2003) have shown that this discrepancy can be resolved if a large proportion of LMXBs are descendants of IMXBs and it is assumed that X-ray active lifetimes are reduced by X-ray irradiation of the donor star.

The general formation scenario for an LMXB starts with a high-mass ($M > 10M_{\odot}$) primary star and a low-mass ($M < 2M_{\odot}$) secondary star in an orbit that is wide enough to allow the more massive star to evolve onto the giant branch before filling its Roche-lobe. Owing to the extreme mass ratio the mass transfer occurs on a dynamical timescale and is highly unstable, so that a common-envelope (CE) results. Two paths from here can be taken; either the two stars do not have enough orbital energy to drive off the CE and coalesce, therefore not producing an LMXB, or, the helium core of the primary and the secondary star survive the spiral-in phase with a smaller final separation than initially. The helium star then evolves to become either a NS or BH, depending on the initial mass of the primary. Finally the secondary star must evolve to fill its Roche-lobe (through its nuclear evolution and/or by angular momentum loss from the system) and initiate stable mass-transfer to the compact companion. This is thought to occur via an accretion disk and the result is a LMXB system. Typically the donor star is thought to be a main-sequence (MS) star but giant and white dwarf (WD) donors are also possible.

Within the prescription based approach of population synthesis there are many uncertainties involved in modelling LMXB formation, not the least being the ad-hoc description of CE evolution (Paczynski 1976). Under standard assumptions for the efficiency of the energy exchange between the orbit and the envelope during the CE spiral-in phase, Portegies Zwart, Verbunt & Ergma (1997) found that the calculated BH-LMXB birthrate was only 1 per cent of the NS-LMXB rate. Kalogera (1999) showed that abnormally high values of the efficiency parameter, α_{CE} , are required to gain any agreement with the observationally inferred BH-LMXB birthrate. More recently Podsiadlowski, Rappaport & Han (2003) included a more accurate description of the CE process by considering the detailed structure of the giant star in calculating the envelope binding energy. However, BH-LMXB formation remained problematic. In this, and the related study of Pfahl, Rappaport & Podsiadlowski (2003) for NS-LMXBs, the X-ray binary mass-transfer phase was modelled using a full stellar evolution code. While representing an important step forward in the modelling approach, the LMXB systems, within Pfahl, Rappaport & Podsiadlowski (2003), were still generated using the traditional Monte Carlo population synthesis technique and aspects such as tidal evolution and the accretion disk were omitted.

An interesting comment was made by Kalogera (1999) that mass-loss from stars during the helium star phase must be less than half of their initial mass if significant BH-MS binary formation is to occur. It now seems that helium star mass-loss rates derived from observations of Wolf-Rayet stars may be too high by a substantial amount (Pols & Dewi 2002). Reducing these rates will lead to increased BH pro-

duction (at the expense of NSs) and will also mean that the post-CE binaries will not expand by as much as the helium star evolves. These factors combined should help in addressing the NS/BH-LMXB birthrate imbalance. Other possibilities such as additional angular momentum loss mechanisms, a change in the assumptions involved in CE evolution, and flaws in the stellar models of massive stars, have been suggested by Podsiadlowski, Rappaport & Han (2003) in response to the BH-LMXB formation problem.

With an up-to-date rapid binary evolution and population synthesis package the aim here is to improve our understanding of low-mass X-ray binary formation. The effects of various model evolutionary parameters and how modification of these can affect model LMXB numbers and formations rates is considered. In particular, for the first time we will look at how alterations to the helium star wind mass-loss rate affects the production of BH-LMXBs. Other factors such as the common-envelope model and the metallicity of the star will also be explored. An advantage of the population synthesis code is that the stellar evolution prescription is not limited to solar metallicity stars. Another advantage is that tidal circularization and synchronization of the binary orbits are followed in detail. This feature has been neglected in previous studies (e.g. Portegies Zwart, Verbunt & Ergma 1997) and is important even for circular binaries as tidal synchronization will continue to affect the orbital parameters. Also tidal forces are necessary to remove any eccentricity induced in a post-SN binary prior to the onset of mass-transfer. Aside from the fact that tidal evolution is a natural consequence of close binary evolution, including a description of tides in population synthesis models is important as it affects timescales and outcomes (Hurley, Tout & Pols 2002).

We are also motivated to make comparisons with previous population synthesis efforts. In particular we would like to address the difficulties these efforts have encountered in matching the observationally derived birthrates and numbers of BH-LMXBs, and the relative formation rates of NS and BH-LMXBs. Here we must be particularly careful in the extent to which we rely on the observational results. Romani (1998) has suggested a plausible range of 1200 to 2400 for the actual number of BH-LMXBs in the Galaxy. We would like to treat this as no better than an order of magnitude estimate, in that it seems much more likely that the Galactic population of BH-LMXBs numbers in the thousands rather than in the range of tens to hundreds. It is this latter range into which the results of previous theoretical studies have fallen.

In Section 2 we describe the binary evolution algorithm and discuss uncertain aspects of stellar and binary evolution that affect the production of LMXBs. Then in Section 3 we take a semi-analytical approach to make initial constraints on the parameter space for LMXB formation and how variation of key evolutionary parameters affects this. Section 4 involves the population synthesis model and the calculations of the formation rates and numbers for NS and BH-LMXBs. The results are discussed in Section 5.

2 BINARY EVOLUTION MODEL AND UNCERTAINTIES

2.1 Rapid binary evolution code

To follow the evolution of a binary system we use the Binary Star Evolution (BSE) code presented by Hurley, Tout & Pols (2002). This package is prescription based, in that the various aspects of the evolution that can be envisaged are dealt with according to the best model or belief for the outcome of that particular process available at the time. This approach has obvious shortcomings compared to following the evolution with a detailed code (Nelson & Eggleton 2001, for example) but has the advantage that it is rapid and robust and thus ideally suited to synthesizing large binary populations. The BSE algorithm models stellar evolution by incorporating the single star evolution (SSE) package (Hurley, Pols & Tout 2000) which is a series of analytic formulae fitted to the output of detailed stellar models. For any given mass, metallicity and age, the SSE algorithm can provide quantities such as luminosity, radius and core mass for a star. This can be calculated for all evolutionary phases from the zero-age main sequence (ZAMS) through to and including stellar remnants. The SSE algorithm also includes a prescription for mass-loss in a stellar wind and follows the spin evolution of the star.

The basic picture of the BSE algorithm involves two stars evolved forward in time according to the SSE prescription. In addition the algorithm needs to check whether the stars interact with one another and account for all possible processes which may affect the orbital parameters. Tidal interactions between the stars and the resulting change in orbital angular momentum and eccentricity are modelled in BSE for convective, radiative and degenerate damping mechanisms. Other processes which can cause angular momentum loss, such as gravitational radiation in close systems and magnetic braking of stars with appreciable convective envelopes, are also included. At each timestep, after the stellar parameters have been updated, all possible changes to the orbital angular momentum are summed, including changes owing to mass variations, and the orbital parameters are updated. The package then checks for the onset of Roche-lobe overflow (RLOF) and repeats the process for the next timestep if this is not the case.

If RLOF does occur the mass transfer timescale is found (dynamical, thermal or nuclear) and, depending on this and other aspects such as the evolution phase of the two stars, the response of the system is calculated. If mass-transfer occurs on a dynamical timescale then depending on the mass-ratio of the stars the response of the system may be to form a CE which is treated as an instantaneous event and the outcome will be either a merger of the stars or a detached binary. As a result the RLOF phase is exited and the stars (or star) are evolved as described above. If mass-transfer is steady then RLOF is an iterative process with the primary losing an amount of mass Δm_1 at each timestep and the secondary accepting a fraction Δm_2 of the matter as calculated by BSE. To determine whether material transferred during RLOF forms an accretion disk around the companion star, or instead hits the companion in a direct stream, BSE calculates a minimum radial distance r_{\min} , of the mass stream from the companion (Ulrich & Burger 1976). If r_{\min} is less than the radius of the accreting star then an accretion

disk is not formed, otherwise it is assumed that the material falls onto the companion star from the inner edge of a Keplerian disk. Total angular momentum is conserved in this model. Orbital changes owing to tides, gravitational radiation and magnetic braking are followed during RLOF and the stellar parameters, such as the stellar radii, continue to be updated. If at the end of the timestep the primary radius is still larger than its Roche-lobe then the RLOF process is repeated, otherwise the binary returns to being treated as a detached system. The interested reader can find full details of the BSE algorithm in Hurley, Tout & Pols (2002).

2.2 Model uncertainties

We next outline some of the uncertainties in the stellar and binary evolution model that impact upon the formation of LMXBs.

2.2.1 The NS-BH mass boundary

In terms of the initial mass of a star it is generally accepted that stars of $9M_{\odot}$ or less will evolve to become WD remnants. For these stars the core remains degenerate on the asymptotic giant branch (AGB) and burning does not proceed past carbon. Above about $9M_{\odot}$ stars will end their nuclear-burning lives in a core-collapse supernova leaving either a NS or BH compact remnant. We note that the actual boundary mass between WD and NS/BH formation depends somewhat on metallicity and the particulars of the stellar evolution model (Pols et al. 1998). Stars initially more massive than about $20 - 25M_{\odot}$ are assumed to evolve to a BH remnant (e.g. Podsiadlowski, Rappaport & Han 2003), corresponding to an AGB core mass of about $7M_{\odot}$ or greater (Hurley, Pols & Tout 2000).

Similar to WDs, neutron stars increase in density as their mass increases in order to generate the higher pressure needed to counteract the effect of gravity. In this way there is an upper limit for the mass of a NS just as the Chandrasekhar mass limit exists for WDs. However, for NSs the upper limit is not as clearly determined as it depends upon the strong force of neutron-neutron interactions, and this is not fully understood. The limit also changes if the NS is spinning because a star supported by both pressure and rotation will be less dense and will have smaller gravity than the same star not rotating. As a result studies place the limiting NS mass in a relatively wide range between 1.5 and $6M_{\odot}$ (Srinivasan 2002).

Another uncertainty in determining the maximum mass of a neutron star and thus the boundary mass between NS and BH formation is the issue of fallback during the core-collapse supernova. Models of core-collapse are somewhat uncertain (Fryer & Kalogera 2001) but an approximate picture is that initially a neutron star remnant forms from the collapse of the compact progenitor, the collapse is halted somewhat by the nuclear forces between the neutrons which are formed within the collapse. This halting of the collapse creates a shock wave that propagates through the outer layers of the star igniting further nuclear reactions and pushing on the envelope of the star. Depending upon the detailed structure of the stellar envelope, the shock will eject the envelope or it will stall and allow some or all of the envelope

to fall back onto the initial neutron star remnant. If material falls back onto the star, then the mass of the remnant increases and possibly leads to the creation of a BH. Studies suggest that progenitors with a ZAMS mass of $20M_{\odot}$ or less do not experience any fall back while masses in excess of $42M_{\odot}$ lead to direct collapse of a BH and intermediate progenitor masses form remnants via partial fallback (see Belczynski, Kalogera & Bulik 2002).

The maximum mass of a NS and the boundary between NS and BH formation are obviously key factors when comparing the ratio of NS-LMXB to BH-LMXB formation. Belczynski, Kalogera & Bulik (2002) found that the SSE prescription for remnant masses was underestimating the NS and BH masses if fallback was taken into account. Thus we adopt their suggested method for calculating the masses and initially assume that $3M_{\odot}$ is the maximum possible NS mass. This corresponds to a boundary initial mass between NS and BH formation of $21M_{\odot}$ for solar metallicity stars (lower for lower metallicity stars which have greater AGB core-mass for a given initial mass).

2.2.2 Supernovae velocity kicks

Except in the case of complete fallback the supernova explosion has an associated impulsive mass loss. If the supernova occurs in a binary the ejected mass will induce an eccentricity into the orbit and may even destroy the system completely (Pfahl, Rappaport & Podsiadlowski 2003). There is also evidence that the supernova remnant receives a velocity kick owing to an asymmetry in the explosion. This comes, for example, from observations of pulsars which have mean velocities of $100 - 200 \text{ km s}^{-1}$, far in excess of the mean for normal stars (Fryer & Kalogera 2001). The final state of a binary system involving a supernova kick depends on the orbital parameters at the precise moment the supernova event occurs as well as the magnitude and direction of the kick velocity and the amount of mass lost (Kalogera 1996). The introduction of a kick generally increases the likelihood that a binary will be disrupted, although Pfahl, Rappaport & Podsiadlowski (2003) make a pertinent point that some systems require a kick of appropriate magnitude and direction if they are to survive the supernova at all. There is uncertainty as to whether or not BHs receive a velocity kick (Podsiadlowski, Rappaport, Han 2003), especially in the case of complete fallback. Observations of systems such as the BH X-ray transient GRO J1655-40 (Willems et al. 2005) which appears to have a large space velocity would seem to indicate that they do although a possible explanation is that the system was originally a NS binary which received a kick and subsequent mass transfer caused the NS to evolve to become a BH.

Unless otherwise stated we will assume that neither NSs or BHs receive a velocity kick at birth. This is in line with previous population synthesis studies (Portegies Zwart, Verbunt & Ergma 1997; Podsiadlowski, Rappaport & Han 2003) and recognizes that we do not fully understand the origin of the kicks or the conditions under which they develop (Podsiadlowski, Rappaport & Han 2003 and references within). Also, allowing velocity kicks at birth for neutron stars and black holes introduces a randomness to the population synthesis process (Kalogera & Webbink 1998) that may blur comparisons between distinct models. This is not to say that

we don't recognise that SN velocity kicks are a physical requirement, especially in the case of neutron star production. In models where we do include the effect of SN velocity kicks we take the kick velocity v_k from a Maxwellian distribution,

$$P(v_k) = \sqrt{\frac{2}{\pi}} \frac{v_k^2}{\sigma_k^3} \exp^{-\frac{v_k^2}{2\sigma_k^2}} \quad (1)$$

with, $\sigma_k = 190 \text{ km s}^{-1}$ as suggested by Hansen & Phinney (1997).

2.2.3 Common envelope evolution

The existence of cataclysmic variables with orbital periods of the order of days but where the progenitor of the WD must have had a radius in excess of the observed size of the binary at some point in the past proved puzzling for many years. The solution, suggested by Paczynski (1976), involves the partial spiral-in of the low mass secondary towards the core of the primary star, both of which are held within the primary stars envelope, i.e. common-envelope evolution. If the spiral-in process halts before coalescence because the envelope is completely driven off, then a close binary system can result. Although we have no direct evidence of such a situation, something like it must be at work in order to produce close binaries containing remnant stars. Modelling of the process is necessarily simplistic and rather ad-hoc and some variation in the model details exists.

Consider a primary star of mass M which overfills its Roche-lobe on a dynamical timescale and results in the envelope of the primary surrounding the secondary star of mass m and the primary core of mass M_c . The secondary star and the primary core will spiral-in towards each other and transfer orbital energy to the envelope with an efficiency measured by the parameter $\alpha_{\text{CE}} = E_{\text{bind}}/\Delta E_{\text{orb}}$. This is the ratio between the initial binding energy of the envelope and the change in orbital energy between the initial and final configurations of the CE phase. If the separation of the stars at the end of the CE, a_f , is such that either the secondary star or the remnant of the primary fill their Roche-lobes then the objects will have coalesced during the process. In the BSE package the binding energy is calculated as that of the giant envelope immediately prior to the onset of the CE,

$$E_{\text{bind}} = -\frac{GM(M - M_c)}{\lambda R} \quad (2)$$

where λ depends on the structure of the primary star. The initial orbital energy is that of the secondary star and the primary core separated by a_i (the orbital separation of the binary at the onset of CE), i.e.

$$E_{\text{orb},i} = -\frac{1}{2} \frac{GM_c m}{a_i}, \quad (3)$$

and the final orbital energy is

$$E_{\text{orb},f} = -\frac{1}{2} \frac{GM_c m}{a_f}. \quad (4)$$

Alternatively the initial configuration can take the binding energy as being between the envelope mass and the combined mass of the primary core and the secondary star (Iben & Livio 1993; Yungelson et al. 1994) which gives

$$E_{\text{bind}} = -\frac{G(M_c + m)(M - M_c)}{a_i}. \quad (5)$$

Another formulation (Webbink 1984; de Kool 1990; Podsiadlowski, Rappaport & Han 2003) calculates the binding energy in the same way as the BSE method but takes the initial orbital energy to be

$$E_{\text{orb},i} = -\frac{1}{2} \frac{GMm}{a_i}. \quad (6)$$

We refer to this as the PRH CE scheme.

In general we use the BSE CE but the effect of the alternative schemes will also be considered, as will the effect of varying α_{CE} . The parameter λ has generally been taken as a constant of value 0.5 in previous studies (e.g. Hurley, Tout & Pols 2002) but it has been pointed out that this may underestimate how tightly bound the envelopes of massive stars are (Dewi & Tauris 2001). Podsiadlowski, Rappaport & Han (2003) have looked at detailed models of massive stars and found that λ can be as low as 0.01 for stars with $M > 25M_{\odot}$. Since the publication of the BSE algorithm, which assumed $\lambda = 0.5$ for all stars, an algorithm that computes λ based on the results of detailed stellar models (Pols et al. 1998) has been added to the BSE package (Pols, in preparation). This allows λ to vary from star to star and as a star evolves. Values of λ for massive stars are in agreement with Podsiadlowski, Rappaport & Han (2003) and we will look at how different assumptions regarding λ affect BH-LMXB production.

2.2.4 Helium star wind strength

After the NS or BH progenitor has filled its Roche-lobe as a giant and had its envelope stripped during CE evolution, the exposed core will evolve for some time as a naked helium (nHe) star before collapsing to become a compact remnant. Mass loss in a stellar wind from the nHe star can be crucial in determining if the final remnant is a NS or BH. Also, if the mass is lost from the binary system then a substantial increase in orbital separation occurs and hinders the likelihood of the binary entering a LMXB phase later in its evolution. In the SSE (and thus BSE) package mass loss from helium stars is modelled using the observationally derived rate

$$\dot{M}_{\text{nHe}} = 10^{-13} L^{1.5} M_{\odot} \text{ yr}^{-1} \quad (7)$$

(Hamann, Koesterke & Wessolowski 1995) where L is the stellar luminosity. Improved wind models have lead Hamann & Koesterke (1998) to suggest that this may be an overestimate of the actual rate by a factor of 3-5 and in fact Nugis & Lamers (2000) have presented a rate which is up to an order of magnitude smaller for typical nHe star masses. In light of this uncertainty we have introduced a parameter μ_{nhe} into Equation 7 which we will use to investigate the effect of reducing the helium star wind strength on LMXB production.

3 CONSTRAINING THE PARAMETER SPACE

Before rushing headlong into a full population synthesis it is helpful to initially constrain the parameter space for LMXB formation. To do this we take a semi-analytic approach that closely follows the method outlined by Portegies Zwart, Verbunt & Ergma (1997; see also Sec. 3.2 of Kalogera & Webbink 1998). The idea is that for a binary of primary mass M

and secondary mass m we can quickly ascertain the range of initial separations a that likely lead to an LMXB phase for that particular system. This is completed for a range of primary masses using the standard set of evolutionary parameters. The standard model may be repeated with the use of alternative parameter values so we may gauge which parameters LMXB formation is particularly sensitive to. We will therefore know which evolutionary parameters to focus on when we move to the full population synthesis study and thus save valuable computational time.

3.1 Method of constraint

First we use the rapid SSE code to evolve a set of massive primary stars with initial masses of $M_0 = 10, 15, 20, 25, 30, 35, 40, 45, 50, 55$ and $60 M_{\odot}$. Quantities of interest such as the current mass M , radius R and core mass M_c , are recorded as a function of the evolution time as well as the mass M_{rem} and radius, R_{rem} , of the nHe star remnant that would result if the envelope of the star was removed at that time. If an LMXB is to form then the primary star must fill its Roche-lobe at some stage of its evolution and initiate CE evolution. The Roche-lobe radius, R_L , is a function of the orbital separation, a and can be calculated using

$$R_L = \frac{0.49a}{0.6 + q^{2/3} \ln(1 + q^{-1/3})} = r_L(q) a \quad (8)$$

(Eggleton 1983) where $q = m/M$ is the mass ratio of the binary. So at any evolution time we can set $R = R_L$ and calculate the orbital separation required for the primary to fill its Roche-lobe at that instant. If the primary star has lost mass in a stellar wind prior to filling its Roche-lobe, and this mass is lost from the binary system, i.e. non-conservative mass loss, then the separation at RLOF will be greater than the initial separation, a_0 , of the binary. The two separations are related by

$$a_0(M_0 + m) = a(M + m) \quad (9)$$

where it is assumed that the secondary does not lose mass. We now have the information required to calculate a_0 as a function of time for a particular M_0 and m combination, emphasizing that a_0 is the upper limit of the initial orbital separation required for the primary to fill its Roche-lobe at that time, or earlier.

As an example we show the evolution of primary radius and a_0 in Figure 1 for the case of $M_0 = 20M_{\odot}$ and $m = 1M_{\odot}$. We have taken $Z = 0.02$ as the metallicity of the two stars. The maximum radius reached by the primary is $1507R_{\odot}$ and occurs at $T = 9.83$ Myr when the star is on the AGB. However, the maximum value of a_0 , denoted a_{max} , occurs earlier at $T = 8.87$ Myr just after the star evolves off the Hertzsprung gap (HG). The radius at this point is $860R_{\odot}$ and $a_{\text{max}} = 1310R_{\odot}$. Obviously, if the initial separation of the system is greater than this value then the binary will remain detached for its lifetime with no possibility of an LMXB phase. Also the primary can not fill its Roche-lobe at a time later than that corresponding to a_{max} as it would already have done so in the past, if this had been possible.

The next step in the evolution pathway for becoming an LMXB is for the binary to survive the CE phase. This occurs if the final separation, a_f , at the end of the CE is such that neither the primary remnant (a nHe star) nor the

secondary star fill their Roche-lobe. We can calculate the minimum possible a_f required for CE survival by first setting $R_L = R_{\text{rem}}$ and $q = m/M_{\text{rem}}$ in Eq. 8 and then repeating this process for the secondary star filling its Roche-lobe. The maximum of the two values is then the minimum possible a_f for the CE to leave a binary system and generally this corresponds to the secondary star calculation (as was found by Portegies Zwart, Verbunt & Ergma 1997). A corresponding initial separation at the onset of the CE can then be calculated using the equations outlined in Section 2.2.3. Combining these for the BSE scheme gives

$$a_i = a_f \frac{M}{M_{\text{cm}}} \left[m \frac{M_c}{M} + \frac{2(M - M_c)}{\alpha_{\text{CE}} \lambda r_L(q)} \right], \quad (10)$$

where $M_c = M_{\text{rem}}$ and $q = m/M$. Here we have taken $R = a_i r_L(q)$ which means we are assuming that the star does fill its Roche-lobe, as was assumed by Portegies Zwart, Verbunt & Ergma (1997). We must then take into account any primary mass loss prior to the onset of CE using Eq. 9 to calculate an initial minimum separation (which we shall call a_{0m}) corresponding to a_i . This is the minimum possible initial separation for the binary to survive the CE and therefore we require $a_{0m} < a_0$ at some point in the evolution of the primary if a CE is to be initiated and survived. If we define a_{\min} as the separation at the point in the evolution of the primary where the condition $a_{0m} = a_0$ is met for the first time then the range of separations between a_{\min} and a_{\max} are of interest for LMXB formation. Clearly, if a system has $a_{0m} > a_0$ at all times then a_{\min} is undefined and there are no possible initial separations that can lead to a successful CE outcome. The evolution of a_{0m} is shown in Figure 1 for the example system and we see that $a_{\min} = 1214R_\odot$ Myr. We thus find that systems starting with $M = 20M_\odot$, $m = 1M_\odot$ and a separation in the range $1214 - 1310R_\odot$ will possibly lead to LMXB formation. This calculation was done using the BSE CE scheme, $\alpha_{\text{CE}} = 1.0$ and $\lambda = 0.5$.

We note that setting $R = a_i r_L(q)$ when calculating a_i from a_f is not formally correct if $a_{0m} > a_0$ because this means that the star does not fill its Roche-lobe for that value of a_i . In effect the binding energy of the CE has been under-estimated in the calculation but the bearing on the final result is not important as these cases are not of interest. Also, for points in the evolution where $a_{0m} < a_0$ (those that define the separation range) the assumption of $R = a_i r_L(q)$ is valid.

For a set of model assumptions the constraint process can be repeated for various primary masses in order to find the range of possible separations where, in later evolution, an LMXB phase may occur. This method is based on a fairly simplified picture of binary evolution and neglects aspects of the evolution such as tides which, if included, would be expected to shift the calculated separation range. However, it should not alter the existence or non-existence of a range, whatever the particular case may be, as tides will affect the calculation of a_0 and a_{0m} in the same way. Processes which act on the post-CE binary are not considered in this semi-analytical calculation and these may conspire against LMXB formation even if a range of possible separations was found. Examples include supernovae kicks and helium star mass-loss which increases the orbital separation. What the semi-analytical process is good for is comparing results when an uncertain parameter in the model is varied as this gives an

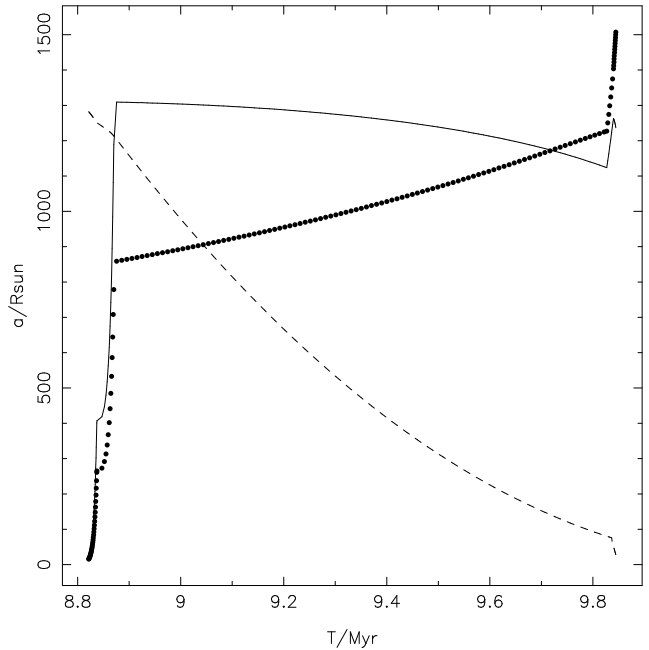


Figure 1. Evolution of radius (solid dots) for a $20M_\odot$ star of solar metallicity. Shown are the HG, core-helium burning and AGB phases. Also plotted are the associated values of a_0 (solid line) and a_{0m} (dashed line) assuming a $1M_\odot$ secondary (see text for details).

excellent indication of what values will work in favour of LMXB formation.

3.2 Constraint results

To compare the predicted separation ranges as a function of primary mass we will first define a standard model which assumes solar metallicity ($Z = 0.02$), a secondary mass of $1M_\odot$, $\alpha_{\text{CE}} = 1$, $\lambda = 0.5$ and the BSE CE scheme.

Figure 2 shows the separation ranges of the standard model for all the primary masses considered. The separation ranges for masses less than $20M_\odot$ are substantially larger than for the more massive stars. The $15M_\odot$ star, for example, has a_0 less than a_{0m} during its HG and core-helium burning (CHeB) phases, so no separation range is contributed here, however, on the AGB a_0 becomes less than a_{0m} with a_0 greater than all previous values. This creates the separation range seen in Figure 2. In contrast the $20M_\odot$ star has a small separation range for LMXB formation while in the CHeB phase but on the AGB a_0 is always less than previous values. Mass-loss truncates the AGB evolution of the $20M_\odot$ star early in the phase whereas the $15M_\odot$ star has a relatively extended AGB lifetime, and can evolve to large radii as a result. The $60M_\odot$ star becomes a nHe star on the HG owing to substantial mass-loss in a wind and has a_0 less than a_{0m} for its preceding HG evolution. This is representative of stars more massive than $50M_\odot$ which evolve too quickly for Roche-lobe contact to be achieved. Portegies Zwart, Verbunt & Ergma (1997) did find a small separation range leading to LMXB formation for these stars but they used a different set of stellar models.

If we switch to using the PRH scheme then the separation at the onset of RLOF is given by

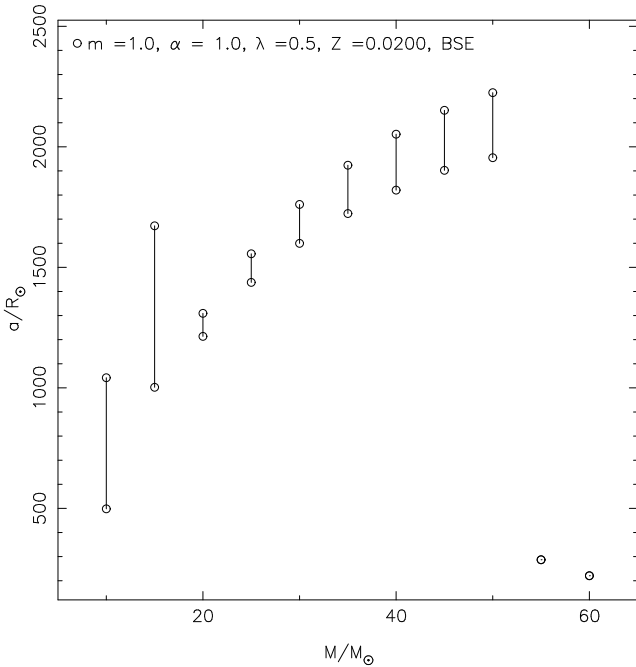


Figure 2. The separation ranges for given primary masses for the standard scenario. We note that for stars where no separation range is produced the point shown is a_{\max} for that star.

$$a_i = a_f \frac{M}{M_c m} \left[m + \frac{2(M - M_c)}{\alpha_{CE} \lambda r_L(q)} \right], \quad (11)$$

which can be compared to Eq. 10 for the BSE CE scheme. This gives separation ranges that are essentially the same as those shown in Figure 2 for the BSE scheme, for all primary masses considered. Some slight differences between the two schemes naturally arise because the primary mass is used in calculating the initial orbital energy for the PRH CE scheme rather than the primary core mass that the BSE CE scheme makes use of. This means that for any given CE scenario the BSE scheme will lead to a greater value of a_f than calculated using the PRH scheme, or conversely a smaller value of a_i (for a given a_f). Basically, owing to the initial configuration of the BSE CE setup it is easier for the cores to drive off the envelope and avoid a merger. However, the choice of scheme does not make a lot of difference to the result.

We next look at how the secondary mass affects the separation ranges for each star. In the standard model we assumed $m = 1M_\odot$ and in Figure 3 we compare this result to that obtained if we instead take $0.1M_\odot$. We see that only the $15M_\odot$ star has a valid separation range when the secondary mass is $0.1M_\odot$. Looking at Eq. 10 we see that a decrease in m leads to an increase in the calculated a_i corresponding to a particular a_f . Thus a_{0m} increases with descending secondary mass. For example, the dashed line in Figure 1 showing how a_{0m} behaves for a $20M_\odot$ primary will be shifted upwards. Conversely, the calculated value of a_0 at any point in the evolution decreases because the mass-ratio used in Eq. 8 is now smaller. This growth in a_{0m} and the decrease in a_0 means that the initial minimum separation becomes less than the maximum initial separation at a later time as compared to the standard scenario. For the primary masses in which no separation range occurs the time delay – which is of the order of 0.3 Myr – is significant enough for a_0

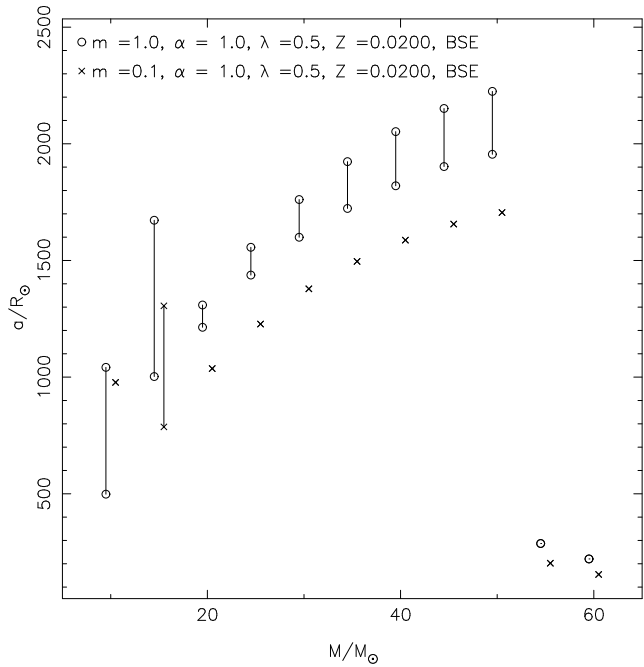


Figure 3. Comparison of separation ranges for given primary masses between the standard scenario and a change to $m = 0.1M_\odot$.

to start decreasing by the time that $a_{0m} < a_0$ first occurs. The difference for the $15M_\odot$ primary star is its extended AGB lifetime where a_0 becomes larger than previous values while also larger than a_{0m} . The lower limit to the separation range has decreased because of the decrease in a_0 corresponding to a particular value of the primary radius. For the $10M_\odot$ star the separation range has disappeared because in this case the decrease in a_0 values ensures that $a_{0m} > a_0$ at all points in the evolution.

Figure 4 exhibits how increasing α_{CE} from 1.0 to 3.0 affects the results. This corresponds to a decrease in the calculated a_{0m} values which leads to an increase in the separation ranges found for all masses. We now see that ranges even exist for the 55 and $60M_\odot$ primaries. On the other hand a decrease in λ (or equivalently α_{CE}) means that the orbit must generate more energy to overcome the envelope binding energy and as a result this makes it more likely that a CE event will end in a merger. As mentioned in Section 2.2, Podsiadlowski, Rappaport & Han (2003) show that λ can be as low as 0.01 during stages of massive star evolution and in Figure 5 we investigate how lowering λ from 0.5 to 0.2 affects the potential for LMXB formation. We see that even this conservative decrease leads to the separation ranges vanishing for all stars except, once again, the $15M_\odot$ star.

Finally we present Figure 6 which compares $Z = 0.02$ and 0.0001 . The major factor producing the separation range differences that we see is that radius evolution for massive stars changes markedly with metallicity. For example, a $20M_\odot$ star with $Z = 0.0001$ has a radius of only $20R_\odot$ when it reaches the end of the HG and the corresponding value of a_0 is $35R_\odot$, much less than for the solar case, while a_{0m} remains high. The low- Z star does not have $a_{0m} < a_0$ until it nears the AGB, with a radius of about $800R_\odot$. So, com-

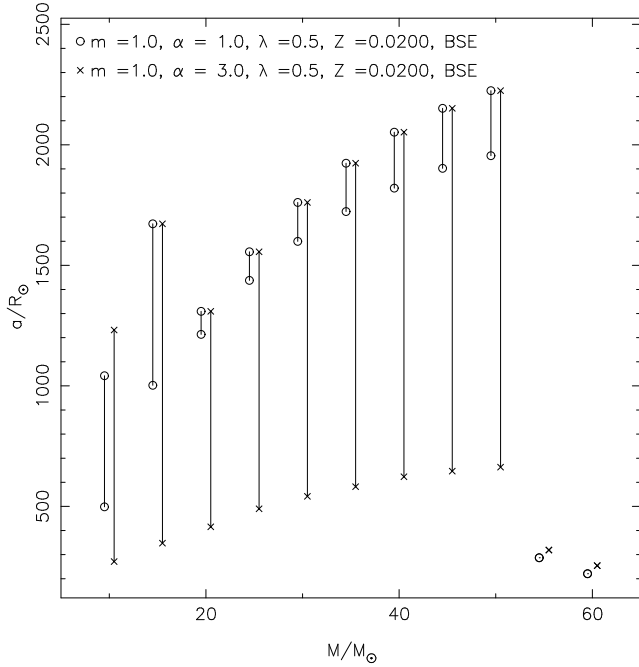


Figure 4. Comparison of separation ranges for given primary masses between the standard scenario and a change to $\alpha_{\text{CE}} = 3$.

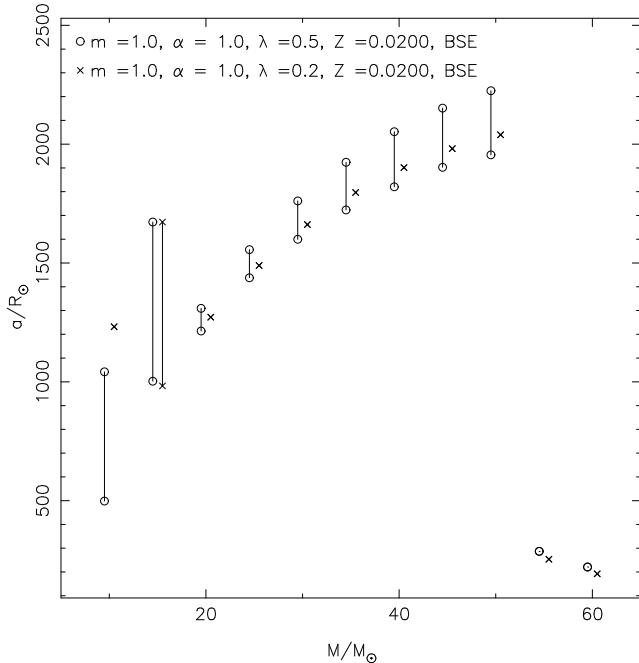


Figure 5. Comparison of separation ranges for given primary masses between the standard scenario and a change to $\lambda = 0.2$.

pared to the solar metallicity star, the separation range for LMXB formation occurs much later in the evolution of the star and leads to an extended range but at smaller separations. For higher mass stars differences in mass-loss rates can also become important. A $40M_{\odot}$ solar metallicity star loses about $5M_{\odot}$ of material in a wind while on the MS compared to only about $0.3M_{\odot}$ for its low metallicity counterpart. So the value of a_0 calculated at similar points in the evolution

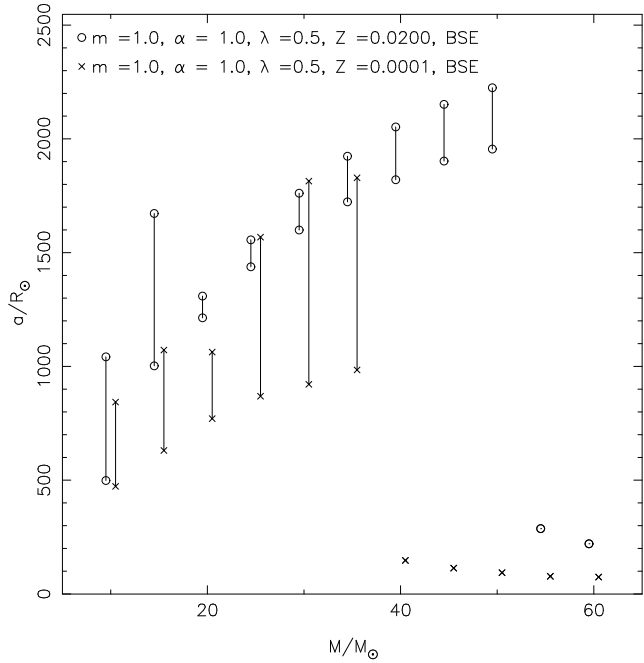


Figure 6. Comparison of separation ranges for given primary masses between the standard scenario and a change to $Z = 0.0001$.

will be smaller for the low-metallicity star, not only because its radius is smaller but also because the mass-ratio used in Eq. 8 will be smaller. For the $40M_{\odot}$ low-metallicity star, and higher masses, we find that $a_{0m} > a_0$ at all points in the evolution, and thus no range is found.

As expected, the common-envelope efficiency parameter has the greatest potential to increase the incidence of LMXB formation. Our preliminary studies have shown that we should not expect significant LMXB formation, especially not BH-LMXB formation, from low values of λ or very low-mass secondaries. This agrees with the findings of Podsiadlowski, Rappaport & Han (2003). The effect of metallicity on the formation rate of LMXBs will also be interesting to study with full population synthesis.

3.3 An evolution example

We next give an overview of LMXB evolution for a particular binary and then illustrate how the evolution changes according to some of the choices made for the parameters of the BSE code. Consider a binary system which involves a primary star with an initial mass of $45M_{\odot}$ and a secondary star with an initial mass of $1M_{\odot}$. The system begins with a period of 1705 days, or approximately a separation of $2150R_{\odot}$, and initially has a circular orbit. The PRH CE scheme is used and the model parameters α_{CE} and λ are assumed to be 1.0 and 0.5 respectively. The metallicity is of solar abundance, $Z = 0.02$.

Initially the evolution of the primary star, relative to the secondary star, is very fast: the MS lifetimes are 4.5 and 10950 Myr respectively. While the massive primary is on the MS it loses $6.5M_{\odot}$ of mass due to a wind and the orbital separation slowly increases as this mass is lost from the binary system, taking angular momentum with it. When the

primary reaches the end of the MS the separation is $2505R_{\odot}$. The primary then evolves quickly along the HG all the while increasing its radius. Only 0.01 Myr after leaving the MS the primary's radius reaches and exceeds its Roche-lobe radius and mass transfer is initiated. The secondary star is still on the MS. At the onset of RLOF the primary has a mass of $38.4M_{\odot}$ and it has just become hot enough for core helium burning to begin – stars initially more massive than about $12M_{\odot}$ can ignite helium while on the HG and effectively do not have a first giant branch (see Hurley, Pols & Tout 2000). The mass-transfer proceeds on a dynamical timescale, which produces a runaway effect, where the entire envelope of the CHeB star (mostly convective) overflows its Roche-lobe and forms a CE around the helium core of the primary and the MS secondary. This is assumed to occur instantaneously. The helium core and the MS star spiral-in towards each other and drive off the envelope before getting close enough to coalesce (see section 2.2.3 for CE description).

The CE phase leaves the binary with a circular orbit and a separation of $6R_{\odot}$. The primary star, now a naked helium MS star, has a mass of $13.6M_{\odot}$ and its radius is well within its Roche-lobe radius. The secondary star, however, is more likely to fill its Roche-lobe now, as the separation has decreased immensely. While the secondary is still on the MS, the primary naked helium MS star evolves onto the helium HG at a system time of 5.2 Myr with a mass of $8.2M_{\odot}$. Shortly afterwards the primary star goes SN. The outcome of the SN event is a $4.7M_{\odot}$ BH primary. The mass lost during the SN is assumed to occur instantaneously and is not enough to disrupt the binary. It did, however, expand the orbit to a separation of $23R_{\odot}$ and induced an eccentricity of 0.58. In this scenario a SN kick for BH formation was not assumed. The mass of the secondary star has increased to $1.06M_{\odot}$ owing to mass accretion from the wind of the primary while it was a helium star.

Jumping ahead to a system time of 11 741 Myr the secondary begins RLOF and the binary is an LMXB. The secondary is on the GB, so the system is not a typical LMXB if the strict classification requiring the secondary to be a MS star is applied. The system is circularised owing to tidal forces acting upon the orbit and at RLOF has a separation of $14R_{\odot}$. Mass transfer occurs on a nuclear timescale and lasts for ~ 300 Myr. The BH mass, in this time, increases to $5.4M_{\odot}$, while the secondary mass decreases to $0.49M_{\odot}$. During the LMXB phase the X-ray luminosity peaked at about $66\,500L_{\odot}$ and the mass-transfer ends when the giant shrinks within its Roche-lobe radius with only $0.01M_{\odot}$ remaining in its envelope. The separation at the end of the LMXB phase has increased to $109R_{\odot}$ and stays, roughly, at this distance for the rest of the system lifetime. The secondary ends up as a white dwarf with a radius well within its Roche-lobe radius.

We note that if we neglect tidal forces for our example binary then the orbit remains eccentric when the LMXB mass-transfer phase begins and the separation between the stars is also greater which means that RLOF actually starts later at a time of 11 909 Myr. The LMXB phase lasts for about 150 Myr which is a factor of two less than when tides are included.

It is interesting and insightful to consider how the evolutionary pathway changes when α_{CE} (or equivalently λ) and μ_{nhe} are varied within this example system. Changing α_{CE}

to 3 gives a wider post-CE binary with a separation of $18R_{\odot}$. Consequently the LMXB phase does not start until a time of 12215 Myr and lasts for only 56 Myr. The final BH mass is $5.3M_{\odot}$ and the mass of the secondary at the end of the LMXB phase is $0.36M_{\odot}$. Decreasing the common-envelope efficiency leads to a tighter post-CE system and increases the chances of a merger occurring during CE. This is equivalent to a decrease in λ , the binding energy parameter, and indeed if we use $\lambda = 0.2$ in our example then the helium core of the primary and the secondary coalesce during CE and there is no LMXB phase. We note that if a velocity kick had been allowed at birth for the BH then the binary would have been destroyed at this time.

We next evolve this example binary according to the standard parameters but with the helium star wind strength reduced by a factor of 5, i.e. $\mu_{\text{nhe}} = 0.2$. Decreasing the wind mass loss from helium stars lessens the increase in the orbital separation during this phase. We now find that when the primary ends its helium star lifetime it becomes a BH of mass $11.9M_{\odot}$ and the separation is only $6.7R_{\odot}$. As a result the secondary fills its Roche-lobe while still on the MS at a time of 1346 Myr and a long-lived classical LMXB phase continues to a time of 15 000 Myr and beyond. It is obvious that reducing the strength of the helium wind is desirable in terms of producing long-lived BH-MS-LMXBs and thus will aid in increasing the formation rate and numbers of the binaries. This will be explored in the next section.

4 POPULATION SYNTHESIS AND RESULTS

With the evolutionary parameters considered in depth, a statistical description of LMXBs is now investigated. This statistical approach is in the form of a full population synthesis and is used to evolve many ($\sim 10^6$) binaries, producing an estimation for the rate of birth of LMXBs and the numbers of these systems in the Galaxy now.

To populate the Galaxy with binaries we first produce a grid of suitable initial parameters (primary mass, secondary mass and orbital separation) and evolve each binary on the grid. For each binary we take into account realistic initial mass functions (IMFs) and period distributions to determine the likelihood of the binary contributing to the Galactic population. Then by picking out the systems that evolve to become LMXBs, and combining this with a star formation rate, we find the birthrate and expected number of LMXBs in the Galaxy. This is repeated for a variety of models.

4.1 Method

A binary system can be described by three initial parameters: primary mass, M , secondary mass, m , and separation, a (or period). A fourth parameter is the eccentricity but it has been shown previously that this has little affect on population synthesis results (Hurley, Tout & Pols 2002). We assume circular orbits here for simplicity. For the primary mass we choose a minimum mass of $5M_{\odot}$ and a maximum mass of $80M_{\odot}$. The lower limit takes into account the requirement that the primary must form a NS or BH to be of interest and $5M_{\odot}$ is considered to be safely below the minimum initial mass for NS formation (noting that we will be evolving some low-metallicity models). As suggested in Hurley, Tout

& Pols (2002) the production of stars with $M > 80M_{\odot}$ is rare when using any reasonable IMF, hence the choice of upper mass limit. We consider secondary masses between the limits of 0.1 and $2.0M_{\odot}$. The upper mass limit in this case is based on the usual definition that an LMXB has a donor star of $2.0M_{\odot}$ or less, while the lower limit is approximately the minimum mass of a star that will ignite hydrogen-burning on the MS. For the initial orbital separation we consider a range between 10 to $3000R_{\odot}$. This choice is guided by the results of the previous section with some leeway at either end. We did maintain a check while evolving each model to see if the upper limit was breached at any point in the binary evolution but even though some LMXB systems were produced from initial separations close to the upper limit, none were produced from binaries with $a_0 = 3000R_{\odot}$. So the choice proved to be fine.

For the primary mass we chose to have 100 grid points and to have these logarithmically spaced so that the grid was finer at lower masses. This gave step lengths of $\Delta \log(M) = 0.012M_{\odot}$. We chose to use 50 grid points for the secondary mass with a linear spacing of $\Delta m = 0.04M_{\odot}$. For the separation we chose 600 steps with $\Delta a = 5R_{\odot}$. This gave a total of 3×10^6 distinct initial parameter sets and each binary on the grid was evolved with the BSE algorithm to an age of 15 Gyr – deemed to be a reasonable upper limit to the likely age of the Galaxy.

To calculate birthrates we must combine our grid of initial parameters with realistic distribution functions in order to calculate the contribution of each binary to the rate. In selecting the form of the initial distributions we are guided by the choices made by Hurley, Tout & Pols (2002) and indeed the process of calculating birthrates and expected numbers follows closely the process described in that work. For the distribution of primary masses we use the power law IMF given by Salpeter (1955),

$$\Phi(M) = kM^{-\alpha}, \quad (12)$$

with $\alpha = 2.35$ and $k = 0.0603$. This is the probability that a star has mass M . There is some uncertainty in the slope of this distribution with Kroupa, Tout & Gilmore (1993) finding that for masses larger than $1.0 M_{\odot}$ a value of $\alpha = 2.7$ is a better fit to solar neighborhood data. The distribution of secondary star masses is not as well constrained and we simply take

$$\varphi(m) = \frac{1}{M}. \quad (13)$$

as previous authors have done (Portegies Zwart, Verbunt & Ergma 1997; Hurley, Tout & Pols 2002). This assumes that the initial secondary and primary masses are closely related via a uniform distribution of the mass-ratio. The initial separation distribution is taken to be flat in $\log(a)$,

$$\Psi(\log(a)) = b, \quad (14)$$

where $b = 0.35993$ is a constant determined by normalization of the distribution between the chosen limits.

For every system which went through an LMXB phase we determine a contribution

$$\Delta r = S \Phi(\log(M)) \Delta \log(M) \varphi(m) \Delta m \Psi(a) \Delta a \quad (15)$$

(Hurley, Tout & Pols 2002) to the overall birthrate. Here S is the star formation rate which we take to be $7.6M_{\odot} \text{ yr}^{-1}$.

This is in rough agreement with Yungelson, Livio & Tutukov (1997) who quote $8.3M_{\odot} \text{ yr}^{-1}$ but note that if the assumed minimum mass of newborn stars is raised from 0.1 to $0.3M_{\odot}$ the rate drops to $4.7M_{\odot} \text{ yr}^{-1}$.

In this manner we calculate the rate of birth for NS-MS-LMXBs and BH-MS-LMXBs by summing the contributions for all binaries that passed through the relevant phase of evolution. We can also estimate the numbers of LMXBs residing in the Galaxy at an age T using

$$N = \sum_j \Delta r_j \times \Delta t_j, \quad (16)$$

where we are sum over all j systems that had an LMXB phase of length Δt_j that began prior to T .

4.2 Models

First we define a standard model which we shall call Model A. This assumes solar metallicity, $Z = 0.02$, a helium wind parameter of $\mu_{\text{nhe}} = 1$ and that the maximum NS mass is $M_{\text{max,NS}} = 3M_{\odot}$. For common-envelope evolution the BSE CE scheme is used in conjunction with $\alpha_{\text{CE}} = 3.0$, and λ is allowed to vary according to the new algorithm added to the BSE package (Pols, in prep.). The change to $\alpha_{\text{CE}} = 3$ for the standard model, compared to the standard scenario used in Section 3 which had $\alpha_{\text{CE}} = 1$, is prompted by our desire to maximize the formation of BH LMXBs. We note that such a value is not unusual (Nelemans et al. 2000) and that Hurley, Tout & Pols (2002) showed that using $\alpha_{\text{CE}} = 3$ in the BSE CE scheme is equivalent to using $\alpha_{\text{CE}} = 1$ in the Yungelson et al. (1994) scheme. A velocity kick is not given to NSs or BHs at birth in the standard model (as explained in Sec. 2.2). The particulars of this model, and all of the population synthesis models that we introduce, are summarized in Table 1.

In Model B we investigate the effect of using the PRH CE scheme. Models C and D differ from Model A by assuming $\alpha_{\text{CE}} = 10$ and $\alpha_{\text{CE}} = 1$, respectively (using the BSE CE scheme). For Model E we lower the maximum NS mass to $M_{\text{max,NS}} = 2M_{\odot}$ in order to quantify how this affects BH LMXB formation. Then for Model F we turn the helium wind mass-loss strength down by a factor of two so that $\mu_{\text{nhe}} = 0.5$. After analysing this initial set of models it turns out that Model F gives much better agreement with observations than Model A (see below) and thus the choice was made to adopt $\mu_{\text{nhe}} = 0.5$ as a standard feature in subsequent models.

In Models G and H we investigate the effect of metallicity; Model G has $Z = 0.001$ while $Z = 0.0001$ is assumed for Model H. Both use $\mu_{\text{nhe}} = 0.5$ so are directly comparable to Model F. Although it is a naive assumption to have all stars within a galactic population born with the same metallicity, comparison of models of various metallicity will at least help in constraining the effect of metallicity upon LMXB populations. The effect of SN velocity kicks are the focus of Model I where we use the kick distribution mentioned in Section 2.2.

4.3 Results and Analysis

In Table 2 we give the rates of birth for NS and BH-MS-LMXBs and the estimated numbers of BH-MS-LMXBs currently in the Galaxy predicted by each of the models. We find that the standard scenario BH-MS-LMXB birth rate is less than 0.1% of the NS-MS-LMXB rate, while the number of BH-MS-LMXB systems produced is only 17. Recalling that we are aiming for BH-MS-LMXB numbers of the order of a thousand then clearly Model A is not suitable. It is this order of magnitude difference (or even greater) between predictions from observation and modelling which we try to address here through reasonable changes in the evolutionary parameters. We also aim to bring the relative birthrates of NS and BH-LMXBs to within an order of magnitude agreement. Tighter constraints than this are not within the scope of the current observations which we use merely as a guide when comparing various models.

As expected from Section 3 and shown in Table 2, switching between the BSE and PRH CE schemes gives negligible difference between the rate of production and numbers of BH-MS-LMXB systems within the Galaxy. This is illustrated in Figures 7 a) and b), which plot the initial orbital separation and primary mass of binaries which initiate a BH-LMXB phase in Models A and B. The systems which are only produced by Model B, when compared to Model A, are generally not BH-MS-LMXBs but rather systems involving NSs. Thus the slight rise in NS-MS-LMXB rates for Model B. There are some additional BH-LMXB systems produced in Model B but these do not contain a MS companion. It must be noted that a NS may accrete enough matter to evolve into a BH and therefore the progenitor mass of the BH may be smaller than the progenitor NS/BH mass boundary. For solar metallicity (both Models A and B) this initial mass boundary is at approximately $21M_{\odot}$, therefore the islands of parameter space below this mass in Figures 7 a) and b) are BH-LMXBs which have formed via accreting NSs.

The analysis of Section 3 showed that a system with a high value of α_{CE} has a greater chance of surviving the CE phase. As an illustration of the effect of this on LMXB production we take the extreme case of $\alpha_{CE} = 10.0$ in Model C. We see that the rates and numbers of BH-MS-LMXBs in Model C are higher than those produced by Model A, as expected. The initial parameter space of binaries in Model C that evolve to become BH-LMXBs is shown in Figure 7c) and the difference compared to Model A is clearly visible. What stands out between these two models is the increase in LMXB systems which form with smaller separations in Model C; there is a $\Delta 1500R_{\odot}$ difference in minimum separation between the $36M_{\odot}$ to $52M_{\odot}$ primary mass range for the two models. The LMXB systems created by Model C that induce the slight increase in BH-MS-LMXB numbers are long-lived BH-MS-LMXB systems. The number of LMXB systems, however, has not risen enough to justify such a large increase in α_{CE} . We stress that using the unphysically high value of $\alpha_{CE} = 10.0$ was merely to illustrate that uncertainty in the common-envelope parameter cannot be utilised to sufficiently raise BH-MS-LMXB numbers. We do not consider this to be a valid parameter change. Looking at Table 2 we see that decreasing α_{CE} to 1 (Model D)

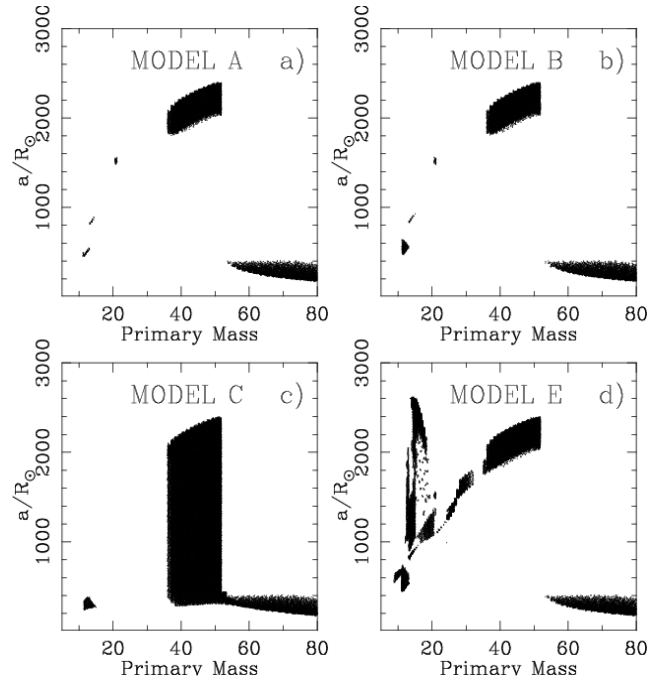


Figure 7. Parameter space of initial separation and primary mass for binaries leading to a BH-LMXB phase in Models A, B, C and E.

means that no BH-MS-LMXB systems are formed. Again, from Section 3, this is not surprising.

Manipulating the boundary of NS and BH formation in Model E obviously has an effect on the numbers of NS and BH-LMXBs produced. Not only is the progenitor NS/BH boundary mass decreased, therefore making it easier to create BHs, but the production of BHs from accretion onto NSs is now greater. The effect on the parameter space of binaries leading to a BH-LMXB phase is shown in Figure 7d) and can be compared to Figure 8a) to see the difference between Models E and A. The progenitor mass NS/BH boundary for Model E is approximately $18M_{\odot}$. Systems with primary masses lower than this are created via accretion onto NSs which then gain enough mass to collapse to a BH and the increase in these systems for Model E simply reflects the decrease in maximum NS mass from 3.0 to $2.0M_{\odot}$. This reduction in maximum NS mass however, does not noticeably affect the birth rate of NS-MS-LMXBs but does increase the rate of BH-MS-LMXBs formation. This change produces satisfying results, the BH-MS-LMXB formation rate is almost within an order of magnitude of the NS-MS-LMXB rate while the number of BH-MS-LMXB systems lies within the predicted observational limits.

Model F which reduces the helium star mass-loss rate also greatly enhances the BH-MS-LMXB formation rate to make it almost within an order of magnitude of the NS-MS-LMXB formation rate. This is similar to the results of Model E and is encouraging. In fact the BH-MS-LMXB formation rate for Model F is a factor of 100 or more greater than we obtained for Model A and is now in the range of 10^{-7} yr^{-1} as indicated by observations (Kalogera 1999). The number of BH-MS-LMXB systems produced by Model F is also very good and well within the estimations from observations (see Table 2). Figure 8 a) depicts the region of

primary mass and binary separation parameter space that involves BH-LMXBs for Model F. This region is not as extensive as in some of the previous models, yet in comparison to these models, Model F produces a much larger proportion of BH-MS-LMXBs. With Model F we find that almost 90% of the BH-LMXB systems produced involve a MS donor star whereas for Models A and E only 15% and 28%, respectively, of the systems shown in Figure 7 have MS secondary stars. Also, the BH-MS-LMXB systems created in Model F are generally long lived, therefore each system makes a greater contribution to the estimated total number. Consider a system with primary mass, $M = 40.8M_{\odot}$, secondary mass, $m = 0.9M_{\odot}$ and separation, $a = 1906R_{\odot}$. In Model A this binary survives the CE phase but the post-CE binary experiences substantial mass-loss both from the primary helium star and during the resulting SN in which the primary becomes a BH. The separation after the SN is about $60R_{\odot}$ and the low-mass MS secondary has no chance of filling its Roche-lobe while on the MS. In Model F however the primary star loses substantially less mass while a helium star and also the mass of the star when it becomes a BH is greater than in Model A. These effects combine to give a much closer post-SN binary with a separation of about $8R_{\odot}$. Subsequently the MS secondary is able to fill its Roche-lobe and a long-lived BH-MS-LMXB phase results. We are much more comfortable with changing the helium wind parameter than we are with altering the maximum NS mass as for the former there is observational evidence suggesting the change (see Section 2.2.4). We now continue by adopting $\mu_{\text{nhe}} = 0.5$ as standard and compare all subsequent models to Model F.

In Model G we assume a metallicity of 0.001 for the stars and we find that the number of BH-MS-LMXBs has increased to 3 290 compared to 1 870 for Model F which assumed solar metallicity. Figure 8b) shows the range of initial parameters leading to BH-LMXBs in Model G and we find that for separations greater than about $1000R_{\odot}$ much more of the parameter space is covered in comparison to Model F. This is because with lower metallicity the massive primary stars suffer less mass-loss from winds so that prior to the CE event there is less increase in orbital separation (see Figure 6). As a result binaries in Model G will be closer than their Model F equivalents and therefore more likely to interact. The radius evolution of the stars is also affected by a change in metallicity and this affects the strength of tidal forces operating in the binaries. There is also a further region in parameter space extending down to $39M_{\odot}$ in primary mass for low separation values, which does not occur in Model F. However, it is a region between $23M_{\odot}$ to $40M_{\odot}$ in primary mass and from $600R_{\odot}$ to $1650R_{\odot}$ in separation where the BH-MS-LMXB systems are created. This region is much larger than that of Model F, which is slightly higher and narrower in separation, resulting in a greater number of long-lived MS-LMXB systems in Model G.

Model H lowers the metallicity even further to a value of 0.0001 and we find that BH-MS-LMXB numbers have now increased to 6 500. The BH-MS-LMXB formation rate is now within a factor of 5 of its NS counterpart. Figure 8c) shows where the BH-LMXBs are created in Model H parameter space. The range in separation for BH-LMXBs, especially those with large primary masses, is increased as compared to both Model F and G. The BH-MS-LMXBs are also extended further down in primary mass to $23M_{\odot}$

rather than $28M_{\odot}$ for Model F. Within Figure 8c) the BH-MS-LMXB systems are found within an area of $23M_{\odot}$ to $40M_{\odot}$ in primary mass and $400R_{\odot}$ to $1300R_{\odot}$ in separation. We also find that there are a greater number of long lived LMXBs in Model H than in Model G. However, the evolution paths of binaries in Model H differ less from what is found in Model G compared to the differences observed between Models F and G. An evolutionary example is given here to facilitate comparison between Models F and H, and to some extent Model G. Suppose a binary involves a primary mass of $M = 31.6M_{\odot}$, secondary mass of $m = 0.95M_{\odot}$ and separation of $a = 1243R_{\odot}$. Within Model H this binary produces a system, which after 6.8 Myr, goes into a CE phase with a CHeB primary of $M = 27M_{\odot}$ and a separation of $1432R_{\odot}$. The binary survives the CE with a separation of $5.7R_{\odot}$. When the primary becomes an $8.6M_{\odot}$ BH the separation is $8.0R_{\odot}$. At a system time of 5 380 Myr the $0.95M_{\odot}$ secondary star evolves to fill its Roche-lobe and a BH-MS-LMXB system is born. After approximately 3 000 Myr the $0.63M_{\odot}$ secondary moves onto the HG ending its MS-LMXB phase. When this binary is evolved in Model F the primary experiences more mass-loss while on the MS which means that the binary is wider than in Model H when the primary reaches the end of the MS. However, the solar metallicity primary has a larger radius and fills its Roche-lobe while on the HG when the orbital separation is $1353R_{\odot}$. A CE phase is initiated but the binary does not survive.

Assuming that all stars within the Galaxy are born with the same metallicity is not the most realistic model as an age-metallicity relation clearly exists (e.g. Feltzing, Holmberg & Hurley 2001). A simple extension of our models is to assume that the metallicity for all stars throughout the Galaxy is some percentage of the three different metallicity values we have used. If we take a mixture of 60% of the stars having $Z = 0.02$, 30% having $Z = 0.001$ and 10% having $Z = 0.0001$ – a somewhat arbitrary choice but in rough agreement with the metallicity distribution for stars in the Galaxy – then with $\mu_{\text{nhe}} = 0.5$ an estimated number of BH-MS-LMXBs is approximately 2759 along with a birth rate of 1.194×10^{-6} . The corresponding NS-MS-LMXB formation rate is 7.61×10^{-6} so the rates are within an order of magnitude which is pleasing. Of course we should correlate the stellar metallicity with the time of birth of each star, and consider a full range of metallicities, and this is something that could be done in the future.

Another uncertain feature, which needs to be tested, is that of the velocity kick given at birth to compact objects. In the models presented so far we have chosen not to include kicks mainly to facilitate comparison with previous work (as discussed in Sec. 2.2). Also, due to the randomness inherent in modelling the velocity kicks neglecting this process makes comparisons between models more transparent. Giving a velocity kick to a star that has passed through a SN phase is, in effect, giving kinetic energy to that star and therefore kinetic energy to the system¹. If the kinetic energy gained is greater than the gravitational potential energy of the system, then that system will become un-bound. Systems with

¹ In cases where the kick is directed in the opposite direction to the orbital motion of the star it is possible for the kinetic energy of the star to be reduced (e.g. Kalogera 1996).

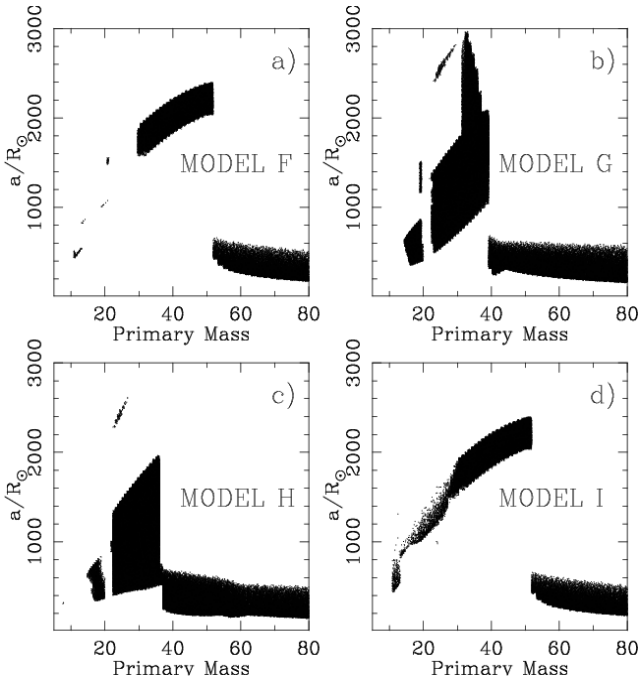


Figure 8. As Figure 7 but for Models F, G, H and I.

low gravitational potential energy (i.e. larger separations) will be disrupted more easily than more strongly bound systems. The impact of allowing a velocity kick at the time of SN is investigated with Model I. What we find is that the ratio of BH-LMXB systems with giant secondaries to those with MS star secondaries declines by a factor of two when going from Model F to Model I. Some of the BH-GB-LMXB systems which have been lost from Model I have instead produced BH-MS-LMXBs. One way in which this may occur is when a system that is too wide to form a BH-MS-LMXB normally has an eccentricity induced via the SN. Tidal forces then circularize the orbit and the separation decreases. In some cases the separation may be reduced sufficiently that the system can evolve to become a MS-LMXB. Alternatively one can imagine that in some systems the kick will widen the orbit to such an extent that mass-transfer does not occur, or occurs later in the evolution than expected for the same binary without a kick. Figure 8d) shows the parameter space in primary mass and orbital separation for Model I and this can be compared to Figure 8a) for Model F. The most noticeable change is the increase in Model I of BH-LMXBs that evolved from NS-LMXBs and this is a direct consequence of the velocity kicks at birth for NSs increasing the likelihood of subsequent mass-transfer.

5 DISCUSSION

In this research we have covered a substantial range of input parameters that affect the outcomes of binary evolution models. The standard scenario, Model A, gives both a poor ratio of birth rate between NS and BH MS-LMXBs and a low number of estimated BH-MS-LMXBs produced within the Galaxy. Both of these results differ to what observations suggest. Portegies Zwart, Verbunt & Ergma (1997) find birthrates of 2.6×10^{-6} for NS-MS-LMXBs and 9.6×10^{-9}

for BH-MS-LMXBs. So results for their standard model are similar to our Model A. It is comforting that models using the same input parameters but different population synthesis codes produce results that are in agreement. However, both standard models give BH-LMXB formation rates much lower than what is indicated by observation. It is therefore a relief that our Models F, E and G give a reasonable match to the observations both for the rate of birth comparisons and actual numbers of systems. We must bear in mind that many areas of binary evolution remain uncertain and within population synthesis there are an uncomfortable number of parameters that are poorly constrained. A prime example is the modelling of the common-envelope phase. What we have been able to show is that no matter which of the algorithms for dealing with CE we use, or what value of the common-envelope efficiency parameter we adopt, it is not possible to make enough BH-LMXBs. So in effect our results are not affected by how the CE is modelled and uncertainty in this parameter becomes redundant. On the other hand we have shown that reducing the amount of mass-loss from helium stars does strongly affect the numbers of BH-MS-LMXB systems created. Simply reducing this by a factor of two from what had previously been used in the binary evolution algorithm – a change that is allowed within the range indicated by observations of Wolf-Rayet stars (Pols & Dewi 2002) – we find that a healthy number of BH-MS-LMXBs are produced in Model F. We therefore suggest that this represents a much better standard model for binary population synthesis calculations.

The results that we have presented up to this point all assume that the age of the Galaxy is 15 Gyr which is a reasonable upper limit. To illustrate how the numbers react to a change in age we have repeated our analysis of Model F but using 12 Gyr for the current age of the Galaxy. These results are given as Model Fb in Table 2 and we see that there is a modest decrease in the birthrates and expected numbers. To investigate how a change in IMF slope affects the results we present a Model Fc which takes a Salpeter (1955) IMF with a slope of $\alpha = 2.7$ as compared to $\alpha = 2.35$ for Model F. In this case we find that the expected number of BH-MS-LMXBs in the Galaxy drops well below what is required to match the observations. Previous studies (e.g. Kalogera & Webbink 1998; Pfahl, Rappaport & Podsiadlowski 2003) have shown that the mass-ratio distribution assumed for the initial binary population can greatly affect the predictions regarding LMXB production. Model Fd in Table 2 is a repeat of Model F but with the assumption that secondary star masses are not correlated with primary star masses – in this case the secondary star masses are given by the Kroupa, Tout & Gilmore (1993) IMF which is a much more accurate representation of the IMF for low-mass stars than the Salpeter (1955) IMF. We see that there is a modest increase in the BH-LMXB birthrate with a corresponding drop in the NS-LMXB rate and that the expected number of BH-LMXBs has roughly doubled. We note that repeating this change in the analysis for Model A only increases the expected BH-LMXB number to 90 (from 17) which is still uncomfortably low.

Another aspect that we need to check is that our choice of grid spacing has not affected the accuracy of our results. If a grid is too coarse, then potentially whole systems of interest may be excluded from the output and obviously we

would like to avoid this. We have performed a Model J which assumes the same input parameters as Model F but uses a higher resolution grid where the spacing in both orbital separation and primary mass are halved. The results are given in Table 2 and are effectively the same as Model F indicating that the results have converged and the size of the grid is not affecting the results.

Pfahl, Rappaport & Podsiadlowski (2003) have suggested that many LMXB systems are evolved intermediate mass X-ray binaries (IMXBs). To allow for this we have performed one final model that extends the secondary mass range to include systems which evolve from secondaries initially more massive than $2M_{\odot}$. This is Model K which deviates from Model F only by taking a secondary mass range of $0.1M_{\odot}$ to $4M_{\odot}$ with the number of grid points increased so that the stepsize of the two models is the same. A system with a secondary mass initially in excess of $2M_{\odot}$ can contribute as an LMXB if the secondary mass drops below $2M_{\odot}$ during mass-transfer. The results for Model K are given in Table 2. The formation rates calculated from this model have increased compared to Model F with the NS-MS-LMXB rate of production being 2.2×10^{-5} and the BH-MS-LMXB rate of production at 9.2×10^{-7} . However, the ratio of NS to BH LMXB birthrates has decreased compared to Model F. The number of BH-MS-LMXB systems has not changed significantly and is now 1910. Within Model K there is a greater range of LMXB production from very high mass primary star systems ($M > 50M_{\odot}$) – these now cover separations between $200 < a < 1400R_{\odot}$. Also, the range of initial separations for systems with a primary mass of $30 - 50M_{\odot}$ has widened to $800 - 2600R_{\odot}$. These are significant parameter space increases when compared to Model F.

Figure 9 compares the distributions of parameter space for Models F and K at the initiation of the BH-LMXB phase. The greater numbers of BH-LMXB systems produced by Model K as compared with Model F can be easily seen. The BH-MS-LMXB region for both models in Figure 9 is at low periods between 0.1 and 1 day and covers 0.2 to $2M_{\odot}$ in secondary mass. Thus the models suggest that BH-LMXBs observed to have periods in excess of 1 d are likely to have sub-giant or giant donors as opposed to MS star companions. We also note that unlike Kalogera & Webbink (1998) we do not need velocity kicks to produce systems with orbital periods less than 1 d. Presumably this is a result of reducing the mass-loss rate from helium stars as well as differences in the modelling of aspects such as common-envelope evolution and tides.

Model K does produce an increase in the numbers of BH-MS-LMXB systems but not by as much as may have been envisaged (e.g. Pfahl, Rappaport & Podsiadlowski 2003). This arises because the BH-MS-LMXB phase lifetimes of the additional systems that evolve from IMXBs are relatively short lived. For example, a system with an initial primary star mass of $46M_{\odot}$, a secondary star mass of $2.4M_{\odot}$ and a binary separation of $1910R_{\odot}$ becomes a MS-IMXB at a system time of 417 Myr, where the secondary star mass has increased slightly to $2.45M_{\odot}$. With the secondary star losing mass to the BH primary its mass eventually falls below the low-mass boundary of $2.0M_{\odot}$ at 660 Myr. This initiates a BH-MS-LMXB phase which ends when the secondary evolves off the MS and results in a phase life-time of approximately 80 Myr. The MS-LMXB phase is only a quarter of the

total X-ray binary life-time. So systems which evolve from IMXBs have higher initial secondary masses than those that start mass-transfer as LMXBs and thus the MS lifetimes are shorter and also time is taken up by the secondary reducing its mass below the $2M_{\odot}$ LMXB cutoff. Previously the IMXB to LMXB formation channel has been utilised to correct for the under-production of standard LMXBs but here this is not necessary as with Model F we already have a healthy MS-LMXB population. The extension to include descendants of IMXBs still gives us a BH-MS-LMXB number that is a good match to the observed range.

In this work we have compared our results to the estimated number of BH-MS-LMXB systems in the Galaxy. This number is based on observations and attempts to account for selection effects and the possible transient nature of the sources. An alternative is to approach the problem from the opposite side and force the population synthesis results to reflect actual surveys – including differentiation between transient and persistent sources. This method would potentially reduce the uncertainties involved in the comparison and help to better constrain the evolutionary parameters. Particularly as most BH-LMXB systems are found to be transient systems as opposed to NS-LMXB systems which are generally persistent sources (van Paradijs 1996; King, Kolb & Szuszkiewicz 1997; Chen, Shrader & Livio 1997). Transient sources have typical outburst times of 100 days while the quiescent phase is of order several years (Truss et al. 2002) and obviously this affects whether or not a system is observable. At present there seems to be two methods to model such transient features in a rapid binary evolution code. These rely on comparing the mass transfer rate via RLOF to a critical mass loss rate (King, Kolb & Szuszkiewicz 1997) or to compare the luminosity of the accretion disk to a critical luminosity (van Paradijs 1996). This is an approach we plan to take in future work but only after producing detailed models of accretion in LMXB systems in order to get a better handle on transient timescales and how these vary with system parameters. The possibility of irradiation affecting transient behaviour will also need to be included (Pfahl, Rappaport & Podsiadlowski 2003). A related extension is to follow the spatial trajectories of the LMXBs within the Galactic potential while also following the binary evolution, as suggested previously by Pfahl, Rappaport & Podsiadlowski (2003). The resulting population can then be surveyed taking into account real selection effects. This will also enable more reliable comparison between synthesized and observed populations.

Finally we mention some alternative theories for close binary formation related to the formation of LMXB systems. These are the triple system scenario (Eggleton & Verbunt 1986) and the tidal capture scenario (Fabian, Pringle & Rees 1975). The triple scenario involves two massive stars in a short-period binary which comprises the inner binary of a triple system with a low-mass dwarf star. The most massive star collapses to a BH but owing to its companion being both close and massive it is likely that the binary remains intact. Eventually the binary components merge to form a BH surrounded by an envelope which expands on a thermal timescale. This envelope engulfs the third star to setup a common-envelope situation in which the low-mass dwarf spirals-in towards the BH. Survival of this CE phase leaves a close binary which may then form an LMXB if the low-mass

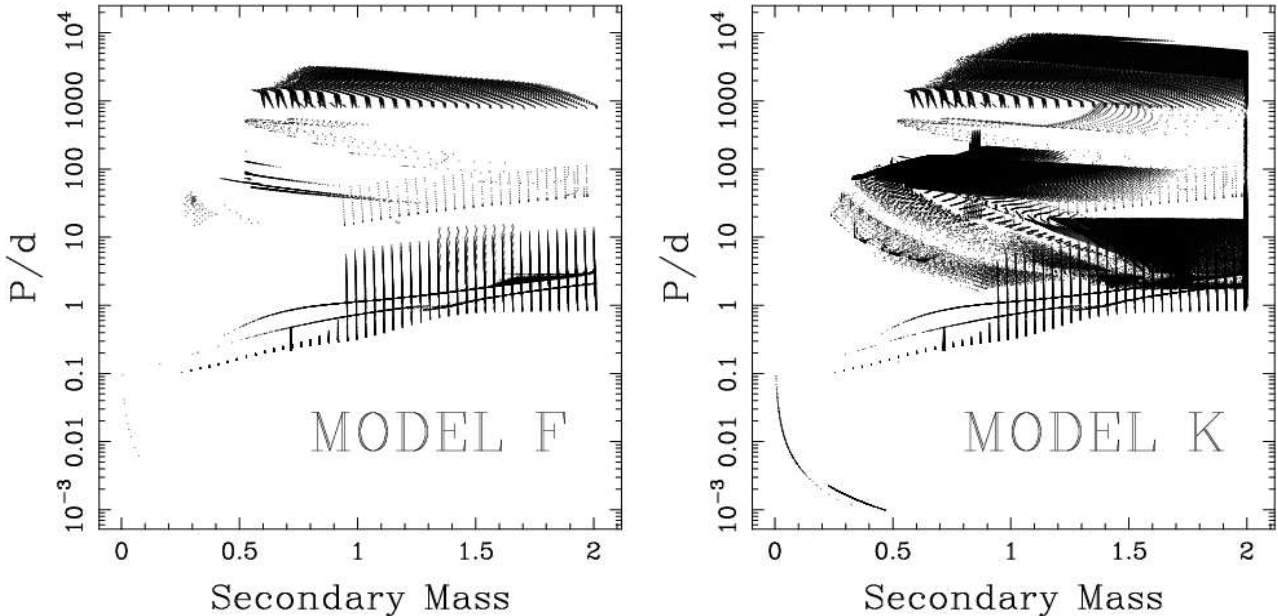


Figure 9. Parameter space of secondary mass and orbital period at the start of the BH-LMXB phase for systems formed in Model F (left panel) and in Model K (right panel). The lined appearance of the points is due to the grid approach of our method.

star subsequently fills its Roche-lobe. The second alternative theory considers a close encounter between a compact object that approaches within a few R_\odot of a non-compact object. During this encounter the gravitational energy between the two stars is absorbed by oscillations produced in the non-compact object. If enough energy is absorbed in exciting these oscillations then the two stars can become bound, and as shown by Fabian, Pringle & Rees (1975) the system created is a close binary. The evolution of the non-compact object may then lead to RLOF and an LMXB phase (if the non-compact object is $< 2M_\odot$). This type of close binary formation is only possible in dense stellar regions, as found in the cores of globular clusters. As Eggleton & Verbunt (1986) explain, the number of close encounters is too small, in the galactic disk or bulge, to account for the numbers of LMXB systems seen. Another possibility that exists in the dense stellar environment of a star cluster is the capture of neutron stars into close binaries through exchange interactions (Hut, Murphy & Verbunt 1991).

6 CONCLUSIONS

To model the Galactic population of low-mass X-ray binaries we have performed population synthesis using a binary evolution algorithm that follows tidal circularization and synchronization of binary orbits. Our favoured model (Model F) estimates that the Galaxy harbours about 1900 LMXBs containing a BH and a MS star companion. The same model predicts the BH-MS-LMXB birthrate to be $4.4 \times 10^{-7} \text{ yr}^{-1}$ and the NS-MS-LMXB birthrate to be $6.5 \times 10^{-6} \text{ yr}^{-1}$. This is in good agreement with the inference from observational surveys that the number of BH-MS-LMXBs residing in the Galaxy is of the order of thousands and that the birthrates of LMXBs with NS and BH components should be comparable. However, we emphasise that these are not robust constraints owing to the uncertainties involved.

To achieve the results of our favoured model we made one simple change to the set of input parameters to the BSE algorithm that had previously been assumed as standard (Hurley, Tout & Pols 2002). Namely we altered the mass-loss rate from helium stars to reflect the improvement suggested by Hamann & Koesterke (1998) over the original prescription of Hamann, Koesterke & Wessolowski (1995) which had until now been adopted in BSE. This amounted to reducing the helium star mass-loss strength by a factor of two. Without this reduction our standard model (Model A) predicted of the order of 10 BH-MS-LMXBs in the Galaxy – failing miserably to match the order of magnitude estimate suggested by observations. This is in line with the findings of previous population synthesis calculations (Portegies Zwart, Verbunt & Ergma 1997; Podsiadlowski, Rappaport & Han 2003) using standard assumptions regarding binary evolution.

We have also investigated the importance of a number of other parameters involved in binary evolution in determining the population synthesis outcome. Varying the common-envelope efficiency parameter, even to excessively large values, does not lead to anywhere near enough BH-MS-LMXBs (Models C and D). Changing the way in which the CE is modelled (Model B) does not improve on the standard model result either. It is actually reassuring that modelling of this ad-hoc process and the choice of the very uncertain efficiency parameter does not have a strong bearing on the results – although obviously a very low efficiency will be detrimental to LMXB production irrespective of the choices made for other parameters. Altering the mass-ratio distribution for the initial binary population (from correlated to uncorrelated masses) does not boost the BH-MS-LMXB numbers of the standard model past 100. As expected we do find that lowering the maximum neutron star mass from 3.0 to $2.0M_\odot$ (Model E) boosts BH-MS-LMXB numbers and gives a good match to the expectations derived from LMXB sur-

veys. However, this change to the model is not as preferable as reducing the helium star wind as for the latter there is observational evidence to justify the change. We find that including LMXBs that evolve from IMXBs is not necessary to explain the observed number of BH-LMXBs but this is a natural evolution sequence and cannot be neglected in these and future calculations.

For the majority of our models we have neglected to impart a kick velocity at birth for the neutron stars and black holes. This was to facilitate comparison with previous studies that took this approach. It also aids in directly quantifying how varying evolution parameters from model to model affects LMXB production. However, for neutron stars at least, there is compelling observational evidence for a velocity kick at birth and this needs to be accounted for in LMXB population synthesis (Kalogera & Webbink 1998). Taking our favoured model and including velocity kicks (Model I) increased the production of BH-LMXBs but did not harm the compatibility of the results. In fact it also gave a NS-LMXB birthrate that compares well with the Galactic birthrate of binary millisecond pulsars. We find that we do not require velocity kicks in order to produce short-period BH-LMXBs.

We suggest that reducing the Hamann, Koesterke & Wessolowski (1995) helium-star mass-loss prescription by a factor of two should be adopted as standard in future population synthesis calculations. Alternatively the weaker rate suggested by Nugis & Lamers (2000) should be used. We also find that varying the initial metallicity of the population can strongly affect the LMXB results and therefore including the Galactic age-metallicity relation in future models would be desirable. Another extension of this work is to model the spatial distribution of LMXBs in the Galaxy. This will allow us to conduct synthetic surveys of the population and compare with raw observed numbers rather than using numbers that have been manipulated to correct for observational uncertainties. In this way we will be able to place stronger constraints on uncertain parameters in the binary modelling process and the results would also be advantageous to observers for understanding existing data and shaping future surveys.

ACKNOWLEDGMENTS

We thank Onno Pols, James Murray and Matthew Bailes for helpful discussions during this work. We are also grateful to the two referees for comments that improved the focus of the work. PDK thanks the Centre for Astrophysics and Supercomputing, Swinburne University of Technology for a scholarship. JRH thanks the Australian Research Council for a Fellowship.

REFERENCES

Belczynski K., Kalogera V., Bulik T., 2002, *ApJ*, 572, 407
 Chen W., Shrader C.R., Livio M., 1997, *ApJ*, 491, 312
 Cowley A.P., 1992, *ARA&A*, 30, 287
 Cowley A.P., Hutchings J.B., Crampton D., Hartwick F.D.A., 1987, *ApJ*, 320, 296
 de Kool M., 1990, *ApJ*, 358, 189
 Dewi J.D.M., Tauris T.M., 2001, in Podsiadlowski P., et al., eds., *ASP Conference Series 229, Evolution of Binary and Multiple Star Systems*. ASP, San Francisco, p.255
 Eggleton P.P., 1983, *ApJ*, 268, 368
 Eggleton P.P., Verbunt F., 1986, *MNRAS*, 220, 13
 Fabian A.C., Pringle J.E., Rees M.J., 1975, *MNRAS*, 172, 15
 Feltzing S., Holmberg J., Hurley J.R., 2001, *A&A*, 377, 911
 Fryer C.L., Kalogera V., 2001, *ApJ*, 554, 548
 Hamann W.-R., Koesterke L., 1998, *A&A*, 335, 1003
 Hamann W.-R., Koesterke L., Wessolowski U., 1995, *A&A*, 299, 151
 Hansen B.M.S., Phinney E.S., 1997, *MNRAS*, 291, 569
 Hurley J.R., Pols O.R., Tout C.A., 2000, *MNRAS*, 315, 543
 Hurley J.R., Tout C.A., Pols O.R., 2002, *MNRAS*, 329, 897
 Hut P., Murphy B.W., Verbunt F., 1991, *A&A*, 241, 137
 Iben I.Jr., Livio M., 1993, *PASP*, 105, 1373
 Kalogera V., 1996, *ApJ*, 471, 352
 Kalogera V., 1999, *ApJ*, 521, 723
 Kalogera V., Webbink R.F., 1998, *ApJ*, 493, 351
 King A.R., Kolb U., Szuszkiewicz E., 1997, *ApJ*, 488, 89
 Kroupa P., Tout C.A., Gilmore G., 1993, *MNRAS*, 262, 545
 Kulkarni S.R., Narayan R., 1988, *ApJ*, 335, 755
 Liu Q.Z., van Paradijs J., van den Heuvel E.P.J., 2001, *A&A*, 368, 1021
 Lorimer D.R., 1995, *MNRAS*, 274, 300
 Nelemans G., Verbunt F., Yungelson L.R., Portegies Zwart S.F., 2000, *A&A*, 360, 1011
 Nelson C.A., Eggleton P.P., 2001, *ApJ*, 552, 664
 Nugis T., Lamers H.J.G.L.M., 2000, *A&A*, 360, 227
 Orosz J., McClintock J.E., Remillard R.A., Corbel S., 2004, *ApJ*, 616, 376
 Paczyński B., 1976, in Eggleton P., Mitton S., Whelan J., eds., *Proc. IAU Symp. 73, Structure and Evolution of Close Binary Systems*. Reidel, Dordrecht, p.75
 Pfahl E., Rappaport S., Podsiadlowski P., 2003, *ApJ*, 597, 1036
 Podsiadlowski P., Rappaport S., Han Z., 2003, *MNRAS*, 341, 385
 Pols O.R., Dewi J.D.M., 2002, *PASA*, 19, 233
 Pols O.R., Schröder K.-P., Hurley J.R., Tout C.A., Eggleton P.P., 1998, *MNRAS* 298, 525
 Portegies Zwart S.F., Verbunt F., Ergma E., 1997, *A&A*, 321, 207
 Ritter H., Kolb U., 2003, *A&A* 404, 301
 Romani R.W., 1998, *A&A*, 333, 583
 Salpeter E.E., 1955, *ApJ*, 121, 161
 Srinivasan G., 2002, *A&ARv*, 11, 67
 Truss M.R., Wynn G.A., Murray J.R., King A.R., 2002, *MNRAS*, 337, 1329
 Ulrich R.K., Burger H.L., 1976, *ApJ*, 206, 509
 van Paradijs J., 1996, *ApJ*, 464, L139
 Willems B., Henninger M., Levin T., Ivanova N., Kalogera V., McGhee K., Timmes F.X., Fryer C.L., 2005, *ApJ*, 625, 324
 Webbink R.F., 1984, *ApJ*, 277, 355
 Yungelson L.R., Livio M., Tutukov A.V., Saffer R.A., 1994, *ApJ*, 420, 336
 Yungelson L., Livio M., Tutukov A., 1997, *ApJ*, 481, 127

Table 1. Characteristics of the main set of models used in this work. The first row gives an identifying letter for each model. In the second row we indicate the value of the common-envelope efficiency parameter and this is followed by the choice of common-envelope scheme. The fourth row shows the metallicity used. Next is the helium wind parameter and the maximum mass assumed for neutron stars. Finally we indicate whether or not kicks were allowed at birth for neutron stars.

Model	A	B	C	D	E	F	G	H	I
α_{CE}	3	3	10	1	3	3	3	3	3
CE scheme	BSE	PRH	BSE	BSE	BSE	BSE	BSE	BSE	BSE
Z	0.02	0.02	0.02	0.02	0.02	0.02	0.001	0.0001	0.02
μ_{nhe}	1	1	1	1	1	0.5	0.5	0.5	0.5
$M_{max,NS}$	3	3	3	3	2	3	3	3	3
Kick	No	No	Yes						

Table 2. Formation rates of NS and BH MS-LMXBs and the predicted numbers of BH-MS-LMXBs in the Galaxy for a variety of models. The age of the Galaxy is assumed to be 15 Gyr in all cases except for Model Fb which assumes an age of 12 Gyr and is identical to Model F in all other respects. Model Fc varies from Model F only by assuming that the slope of the Salpeter IMF is 2.7 as opposed to the value of 2.35 used otherwise. Model Fd varies from Model F by assuming that the secondary mass is drawn independently from the Kroupa, Tout & Gilmore (1993) IMF. Model J is the same as Model F except that a finer grid is used and Model K allows for LMXBs to be descendants of IMXBs.

Model	MS-LMXB rate/yr ⁻¹		Number
	NS	BH	
A	6.4×10^{-6}	3.1×10^{-9}	17
B	9.5×10^{-6}	3.1×10^{-9}	17
C	4.6×10^{-6}	4.3×10^{-8}	220
D	1.5×10^{-6}	0.0×10^{-0}	0
E	6.3×10^{-6}	4.6×10^{-7}	1470
F	6.5×10^{-6}	4.4×10^{-7}	1870
Fb	5.5×10^{-6}	4.1×10^{-7}	1340
Fc	1.6×10^{-6}	6.6×10^{-8}	280
Fd	2.8×10^{-6}	5.3×10^{-7}	4060
G	5.7×10^{-6}	1.7×10^{-6}	3290
H	2.0×10^{-5}	4.2×10^{-6}	6500
I	2.2×10^{-5}	1.0×10^{-6}	6130
J	6.2×10^{-6}	4.4×10^{-7}	1860
K	2.2×10^{-5}	9.2×10^{-7}	1910

This paper has been typeset from a $\text{T}_{\text{E}}\text{X}$ / $\text{L}\text{A}_{\text{T}}\text{E}_{\text{X}}$ file prepared by the author.